CEIG - Spanish Computer Graphics Conference (2024)
J. Marco and G. Patow (Editors)

Enhancing Medical Diagnosis and Treatment Planning through Automated Acquisition and Classification of Bone Fracture Patterns

F.D. Pérez-Cano[1], G. Parra-Cabrera[1], R. Camacho-García[2] and J.J. Jiménez[1]

[1]Department of Computer Science, University of Jaén, Jaén, Spain
[2] University of Jaén, Jaén, Spain

Abstract

The extraction of the main features of a fractured bone area enables subsequent virtual reproduction for bone simulations. Exploring the fracture zone for other applications remains largely unexplored in current research. Recreating and analyzing fracture patterns has direct applications in medical training programs for traumatologists, automatic bone fracture reduction algorithms, and diagnostics. Furthermore, pattern classification aids in establishing treatment guidelines that specialists can follow during the surgical process.

This paper focuses on the process of obtaining an accurate representation of bone fractures, starting with computed tomography scans, and subsequently classifying these patterns using a convolutional neural network. The proposed methodology aims to streamline the extraction and classification of fractures from clinical cases, contributing to enhanced diagnosis and medical simulation applications.

CCS Concepts

• ***Computing methodologies*** → ***Artificial intelligence; Machine learning; Computer graphics;***

1. Introduction

The increasing global trend of an aging population calls for renewed attention to fracture studies. As people age, the natural wear and tear on their bones significantly increases the risk of fractures [CGK*07]. Over the years, as bone fragility increases, a fracture of this type becomes an injury with a significant increase in mortality and sequelae for the population. In depth analysis of these fracture patterns is crucial to better understand their clinical implications and establish effective treatment strategies. Timely and accurate assessments directly contribute to improved patient recovery outcomes. In particular, hip fractures, which are common in the elderly population, carry a significant mortality risk, with rates ranging from 5% to 10% in the first month and progressively increasing throughout the recovery period [SPB*14].

The intricate analysis of bone fractures plays a crucial role in various medical disciplines, from surgical planning and training to diagnosis and treatment optimization. Identifying fracture patterns accurately is paramount for these applications. The classification of these patterns are decisive in determining the treatment and the way in which a patient's recovery is managed. However, current approaches often involve manual processes that are time-consuming and prone to human error.

The aim of this work is the acquisition of fracture patterns by advanced image analysis techniques and their subsequent classification using a convolutional neural network (CNN). This approach will allow automating part of the process, improving accuracy and reducing the time and effort needed to analyze fracture patterns. The results obtained have the potential to cause progress in different areas such as: medical diagnosis, training programs for new traumatologists, automatic fracture reduction systems or more robust treatment planning.

The structure of the article is as follows: firstly, a review of previous literature has been carried out to analyze the latest scientific advances in bone fracture acquisition and classification. The method used to classify the fracture pattern, as well as the procedure for obtaining the fracture images, will be described in the following section. We show the results obtained and discuss about them in the following section. Finally, the conclusions and future work are presented.

2. Related Work

In a previous study, Pérez-Cano et al. [PCJPMV*23] studied the repeatability of a fracture pattern in human femurs within a controlled environment and concluded that, although the characteristics are unique and the shape of the bones varies slightly, they share fragility in the same areas and the conditions can be reproduced to simulate the same type of fracture. These conclusions explain the reason why most of the classifications of bone fractures are based on the zone in which they occur, in addition to the shape of the fractures [Pau36, Gar61, MKNS90, MAR*18]. Medical experts can

DOI: 10.2312/ceig.20241140

use it to establish a diagnosis or prepare a strategy for surgical intervention. Thus, the classification of bone fracture patterns is very useful to improve the decision making.

Bones have a collection of material structures, at multiple scales, which provide a variety of mechanical and biological functions such as providing structural support, protection of organs and mineral storage. Two main types of bone tissue exist: cortical and trabecular. Cortical bone, or dense bone, constitutes a robust outer shell, enhancing bone stiffness and strength. The trabecular bone, or spongy bone, occupies interior spaces and plays a crucial role in energy absorption [SNHJ16]. Therefore, studies that focus on the analysis of bone fractures focus on the cortical part since it is the densest part and the one that supports the load of individuals. In addition, cortical bone is the one used in the clinical setting as it can be analyzed through images obtained from X-Ray and computed tomography (CT) scans.

In recent years, several authors have used advanced deep learning methods to identify features in medical images. This has led to improvements in terms of reduction of pre-processing steps with no manual feature extraction [EKAK17, SWS17]. In [Bu16], the authors developed an automatic diaphyseal femur fracture classification method for the first time. Fractures were classified according to the AO/OTA classification [MAR*18] with an accuracy of 89.97% for nine classes. The main problem of this approach is the large amount of user interaction during the whole process for fracture classification. Some works also implementing a CNN for binary fracture identification [CLDMPB19, YR20] .In [SPH*19], the authors use CNN to divide fractured zones from non-fractured zones to improve manual segmentation through X-ray images. Yoon et al. [YHKJEO20] also classifies fractures fractures according the AO/OTA obtaining an accuracy of 97% in a binary classification while an accuracy of 90% for 10 fracture subgroups. In [VA23], the authors also present a generic purpose model to identify or classify whether an area of a bone is fractured or not using X-ray images. Most literature focuses on the use of X-ray images because they are easier to obtain and only determine whether a zone is fractured or not, without actually identifying the type of fracture as it requires a much more exhaustive process of analysis.

In order to train these advanced models for automatic fracture pattern classification, it is necessary to prepare a set of fracture patterns. In the literature we can find several approaches to obtain the fracture zone from the images of a real clinical case. The procedure to obtain the fracture patterns usually consists of two stages: segmentation of the bone model through CT images and analysis of the fractured area to obtain the pattern using advanced image processing techniques.

The literature segmentation techniques can be divided into two groups: threshold based and region growing based methods. Thresholding methods are characterized by their simplicity and computational efficiency, relying on a predetermined intensity threshold to classify pixels into bone and non-bone regions [NBW*05, TKK*10, VSY*19]. Although they are suitable for images with clear intensity differences, they may fail when intensity variations within bony structures are slight so the authors often include additional filters to improve results. On the other hand, region-growing methods dynamically expand from seed points, adapting to intensity variations and demonstrating resilience to noise [FSH10, PJP14, RSH19]. However, their computational intensity, sensitivity to seed selection, and the need for parameter tuning can be limiting factors that the user needs to configure. 3DSlicer [FBKC*12] is an image computing platform which contains a collection of tools widely used in medical image processing that allows the segmentation of different tissues. This platform contains all the methods mentioned above. In recent years, new techniques have also emerged for the automatic segmentation of CT images using deep learning methods [CLZ*19, MEvE*22].

Once the model is obtained, the 3D bone models are processed to locate candidate points for fractured area identification. Chowdhury et al. [CBRY09] identify fracture surfaces in craniofacial fractures but it involves a costly manual process. Willis et al. [WAT*07] perform a binary classification that allows separating intact and fractured zones of each bone fragment. Other authors present a curvature-based procedure to obtain fracture lines in each slice [OIK*09, KJ13]. Fürnstahl et al. [FSG*12] use a normal-based filter to identify points candidate to belong to the fracture surface. In [LLJPPCJD21, LLPCJD21], the authors use an oriented bounding box and a grid to determine the candidate points. They also use filters based on curvature and statistical parameters to remove outliers. Zeng et al. [ZWX*23] introduce a density-based clustering algorithm to automatically detect the fracture zone.

Therefore, based on our knowledge, we have pioneered the development of an automatic bone fracture model that can classify different types of fracture for long bones using a CNN model trained with precise fracture patterns. The accuracy of the classification results is fundamental, so advanced image analysis techniques have been used to extract fracture patterns with high level of detail from real clinical cases. In the future, the results will benefit the increase the chances of accurate surgical treatment choices to allow early patient mobilization. The model can be extended to the automatic generation of new fracture patterns to use in future tools such as those aimed at training of novice orthopedic surgeons.

3. Methodology

This section contains a detailed description of the fracture patterns selected for classification as well as the methodology followed to obtain these patterns from clinical cases and their subsequent classification.

3.1. Fracture classification

To classify fracture patterns, it is necessary to train the model with representations of these types of fractures. Various fracture patterns have been used following one of the most widespread fracture classifications. [EKZ10] determined that bone fractures can be classified into 7 different kinds:

- Greenstick fracture: a portion of the bone breaks but not completely.
- Transverse fracture: is one that occurs at a 90-degree angle, straight across the bone.
- Oblique fracture: occurs when the bone breaks at an angle.
- Spiral fracture: is the result of the forceful rotation or twisting of a limb.

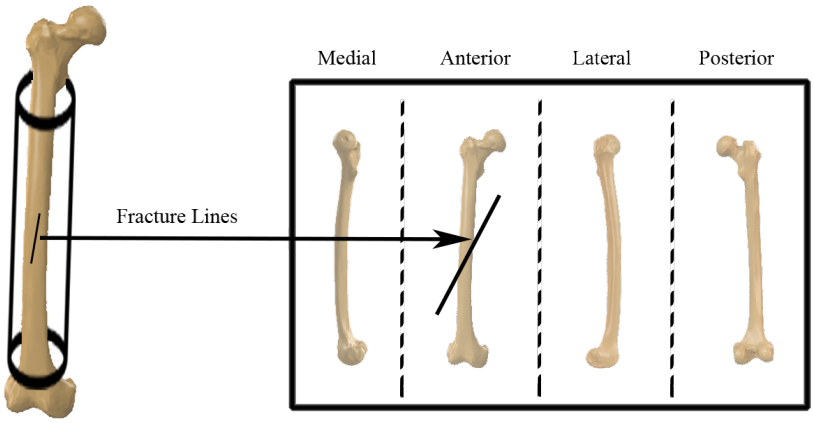

Figure 1: *Representation of the fracture lines in the diaphysis area in a plane using the similarity of the area with a cylinder. In this case, a fracture line affecting only the anterior aspect of the bone is depicted. A complete fracture of the bone would involve fracture lines running through all aspects.*

- Avulsed fracture: is a break at the site where bone attaches to a tendon or ligament.
- Segmental fracture: is a fracture composed of at least two fracture lines that together isolate a segment of bone.
- Comminuted fracture: divides the bone into several fragments.

The AO/OTA classification [MAR*18] was initiated by Müller et al. in 1990 [MKNS90] and adopted by the Orthopedic Trauma Association (OTA). This classification proposes a division of types similar to that shown above in which patterns such as butterfly and linear are also found but omits partial cracks such as Greenstick. Therefore, in order to generalize as much as possible when classifying fracture patterns, the fracture types as presented in [EKZ10], along with the butterfly and linear types of fractures as defined in [MAR*18]. Butterfly fractures, resembling a butterfly shape on imaging, occur in the distal femur or proximal tibia due to axial loading. Linear fractures are characterized by a straight line running across the bone, often indicating a break along the long axis of the bone. A total of 9 different fracture patterns will be used: greenstick, transverse, oblique, spiral, avulsed, segmental, comminuted, butterfly and lineal.

3.2. Clinical case extraction and fracture pattern generation

Given the difficulties in obtaining sufficient images of real clinical cases to extract the fracture pattern needed to train our model, we have combined the extraction of real clinical cases with the use of a tool for automatic fracture pattern generation. For the extraction of the clinical cases we used the 3DSlicer platform [FBKC*12] for the segmentation of the clinical cases. We had to adjust the parameters of the algorithms used during segmentation to the specific case. We have focused on the region growing technique because fractured areas often contain noise. In addition to the fragments that make up the fracture, there is usually detachment of many parts of the bone of a very small size that hinder the process. In addition, we have also used generated island removal and smoothing algorithms to improve the quality of the 3D fracture model. Regarding the identification of the fracture zone for the extraction of the pattern, we followed the technique proposed by Luque-Luque et al. [LLJPPCJD21]. The algorithms that allow the zone to be identified most accurately are those in which the methods combine the use of curvature and normal filters so we decided to use a method to follow these approaches. In addition, the filter based on the growth of regions proposed by the author significantly minimizes the outliers identified as part of the fracture and significantly minimizes the time to clear these points. Once the points that make up the fracture pattern have been identified, it is necessary to determine the best way to store the fracture pattern information. Cohen et al. [CKM*16] proposed in 2016 a representation of the fracture pattern in the distal area involves establishing a similarity between a cylinder and a bone. In addition, after making this approximation, the representation can be projected onto a plane, simplifying its representation. In this plane, the fracture information is represented in the four aspects of the bones (medial, anterior, lateral and posterior). Parra-Cabrera et al. [PCPCJD22] describes an algorithm to approximate the geometry of the bones in the area of the diaphysis to a cylinder and to be able to project these planes later on a plane. Figure 1 shows a diagram of how this representation of the bone works and how it is transformed from the 3D model to the plane. In this case, a fracture line affecting only the anterior aspect of the bone is depicted. A complete fracture of the bone would involve fracture lines running through all aspects. This representation is based on resembling the geometry of the bone to that of a cylinder in order to project the lines defining a fractured area onto a plane and obtain a 2D representation of the fractured area. It is being widely used in recent years as it allows to analyze in great detail the characteristics of the fracture in each part of the bone [CKM*17a, CKM*17b, JDPCPCLL20, PCPCJD22].

Once the fracture zone of the clinical case has been obtained, it is necessary to process it in order to extrapolate it to the previously mentioned representation. For this purpose, the entire fracture zone

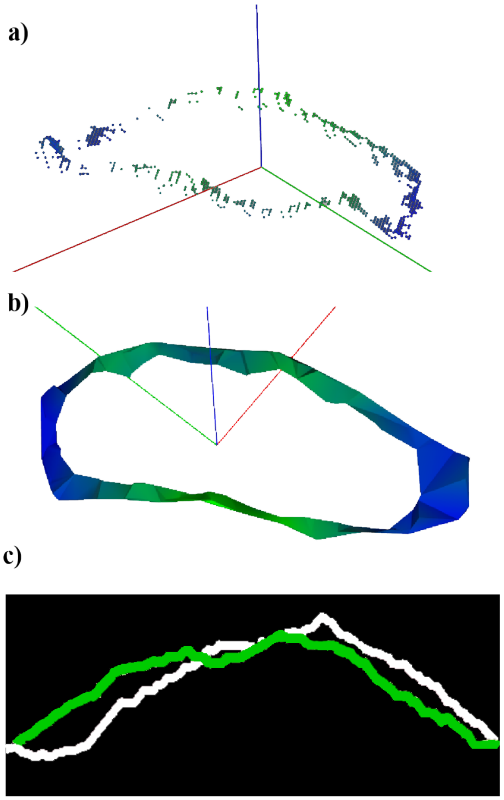

Figure 2: *Process to transform a point cloud with a fracture zone to two-dimensional representation. Figure a shows the point cloud representing the fracture zone, b the triangle mesh representing the fracture and c the result after identifying and projecting the inner and outer contour of the fractured zone into a 2D plane. The white line represents the outer boundary and the green line the inner boundary. .*

has been triangulated and the outer boundary has been extracted to project onto the plane. As the bones are hollow inside, the fracture zone can be represented by the outer and inner borders, delimiting the fractured area of this geometry though a line. Next, the projection allow to represent the fracture lines that make up the fracture in each aspect of the cortical bone. For this purpose, the shape of the bone is resembled to a cylinder and the fracture boundaries lines identified previously are projected onto a plane to obtain a 2D representation. Figure 2 summarizes the process to transform the point cloud identified as fracture zone to a 2D plane. Figure 2c shows the fracture pattern obtained after process the bone fracture area using following the representation proposed by Cohen [CKM*17a].

3.3. Automatic generation of fracture patterns and preparation for training

Since many aspects such as the orientation and aspect in which fracture lines occur are very important in characterizing a fracture pattern and considering it valid, most data augmentation techniques cannot be used to increase the training dataset. They would add noise and worsen the results as each part of the pattern represents an aspect of the bone. Thus, as mentioned above, an automatic fracture generator based on forensic analysis has been used to generate enough fracture patterns to train the deep learning model. [PCPCJD22] developed fracture pattern evaluation and automatic generation of fracture patterns using a set of rules. These rules were formulated by considering various parameters, including the distribution of fracture lines comprising the pattern, the quantity of fracture lines present, their shapes, and the orientations of these fracture lines. The intention behind incorporating these parameters is to create a comprehensive set of guidelines that can effectively describe and analyze the intricacies of the fracture pattern. By taking into account factors such as distribution, quantity, shape, and orientation, the rules aim to enhance the precision and depth of understanding when assessing and characterizing fractures. In our case we have only used the tool for automatic generation to augment the training dataset. After this procedure we start the training with a dataset of 2175 images of 1308x660 pixels. The distribution of images by fracture type is similar. Out of the total dataset, the 30% of the images depict real clinical cases, while the remaining images have been synthetically generated. All images, whether real or synthetic, share the same features. The synthetic images are generated based on forensic analysis using a specialized tool designed to evaluate real fractures described above. Figure 3 shows some of the patterns used to train the CNN model. The lineal and traverse pattern are extracted from clinical cases while the others are synthetic.

3.4. Neural network architecture

Shallow neural networks in classical settings typically consist of three layers: an input layer, a single hidden layer, and an output layer. This is primarily due to the challenge classical learning methods face in converging on deep network structures [WLW*15]. These methods often encounter issues related to gradient vanishing, wherein the gradient values approach zero during iterations, making it challenging to update the parameters in the network. As a result, the training process becomes difficult, and the model struggles to learn effectively in deeper architectures.

The architecture proposed by Krizhevsky et al. [KSH12], also known as AlexNet, is one of the most recognized and used architectures within the scientific community. Its performance for image classification is superior to all other previously proposed methods and served as the basis for the complex deep learning models currently proposed. AlexNet's structure has 60 million parameters and 650,000 neurons. In [LLZ19] discusses the layered structure of this network and highlights why it works so well in image classification. Therefore, taking advantage of the great results that this structure gives when classifying images, we have used this structure to train our model for the classification of bone fracture patterns. The weights of the trained model can also be used.

Since the patterns are represented with black and white images, we replaced the first layer of the original architecture to use only one channel. In addition, to improve memory management, the performance of the model and since the level of detail is not too relevant, we have resampled the size of the images by half (654x330pixels). The last layer of the model has also been modified to accommodate the 9 different types of fracture patterns de-

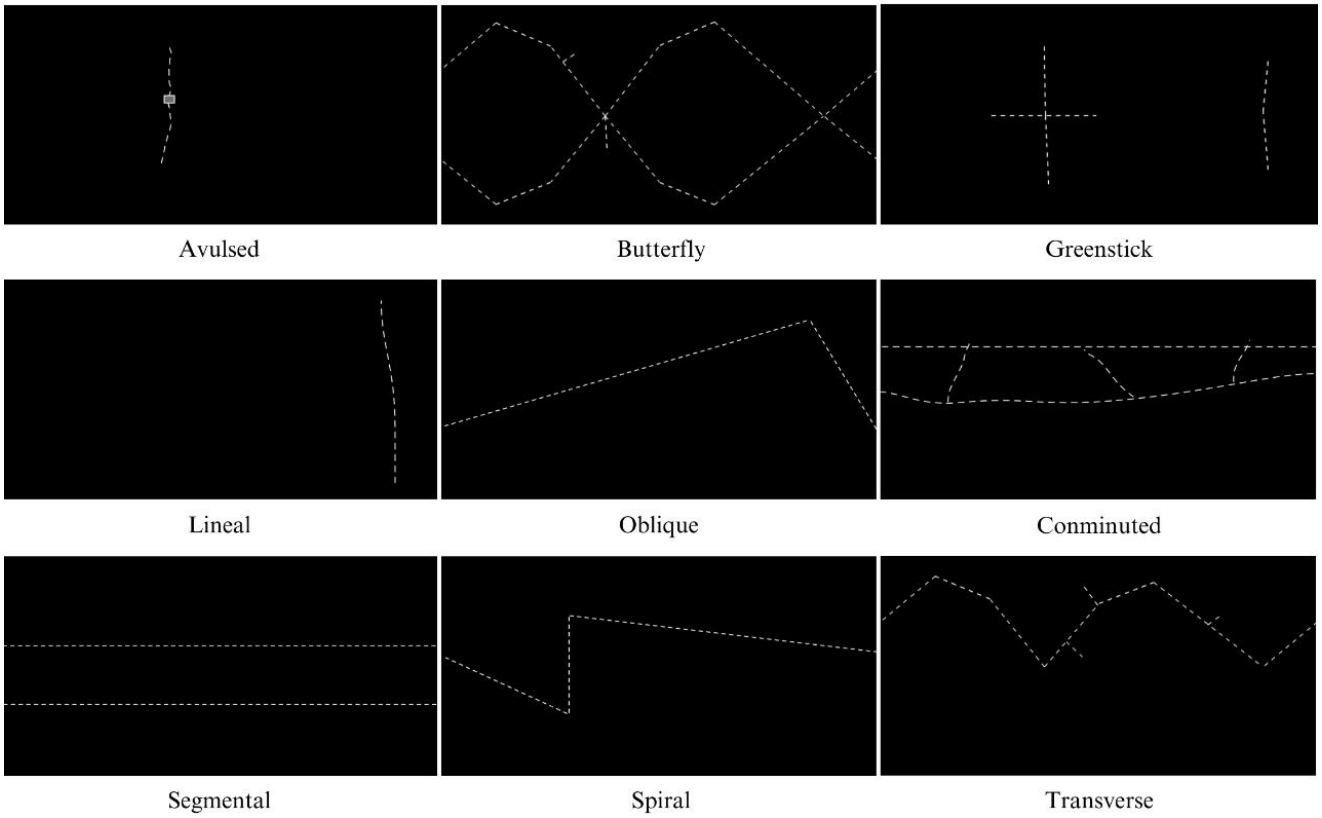

Figure 3: *Fracture patterns generated and ready for model training. The white lines represent fracture lines. The distribution of the lines along the bone follows the same distribution as determined in Figure 1, although they are not visible to avoid noise in the image during the training step.*

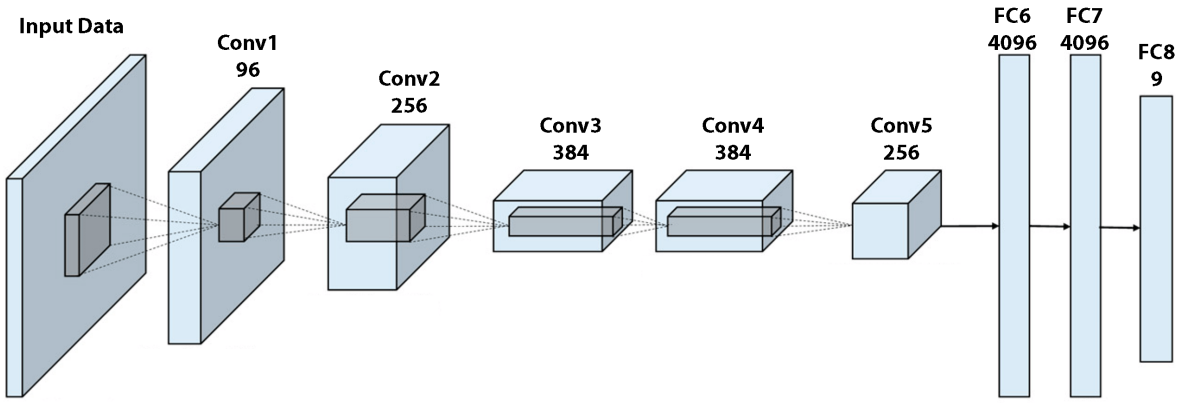

Figure 4: *AlexNet architecture. Includes 5 convolutional layers and 3 fullyconnected layers.*

scribed above. After the modifications, the model has 57 million parameters. Figure 4 represents the structure of the deep learning model trained for bone fracture classification.

4. Results and Discussion

The model has been trained on Pytorch with Intel Core i7-8700 3.20GHz with 6 cores and NVIDIA GeForce GTX1060Ti 6GB GPU. The trained structure can be run on any personal computer. We have used 70% of this dataset for training, 20% for tests and the rest 10% for validation. The training data are used to train the learning model, validation set to fine-tune hyperparameters and the test set to evaluate the performance of the model for the classification of bone fractures. After that division, 1522 images were used to train, 218 to validate and 435 to test the model.

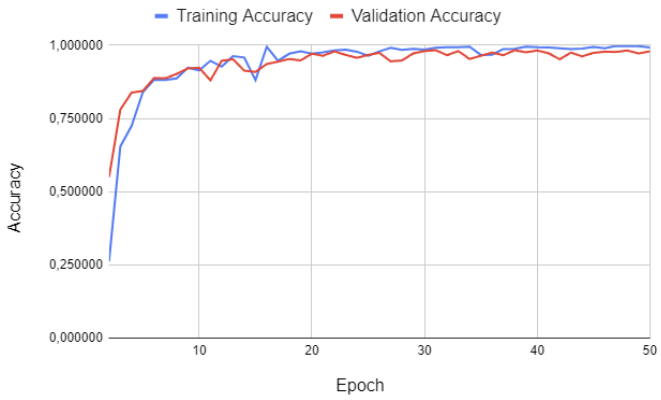

Figure 5: *Train and validation accuracy.*

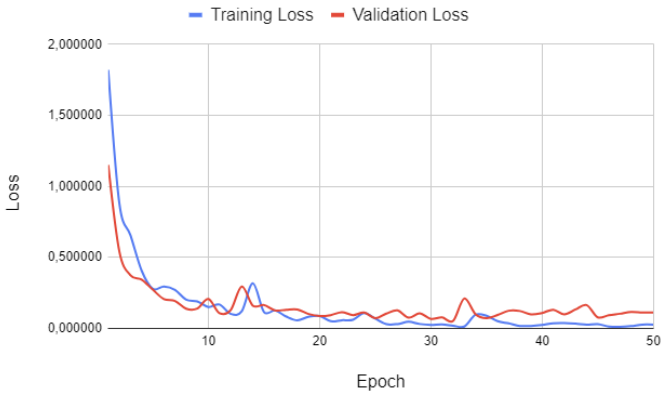

Figure 6: *Train and validation loss.*

The training progress and the result are presented in figures 5 and 6. Figure 5 shows the accuracy while figure 6 shows the loss. The model trained achieved a 0.973 of accuracy in the last epoch. As can be seen in both graphs there is no over fitting since both loss and accuracy during validation and training evolve steadily to the target value. However, if we look at the graph we can see how from epoch 30 onwards the growth is minimal, so it could have stopped earlier.

Figure 7 shows the confusion matrix with the results obtained for each fracture pattern. The segmental fracture and the spiral fracture

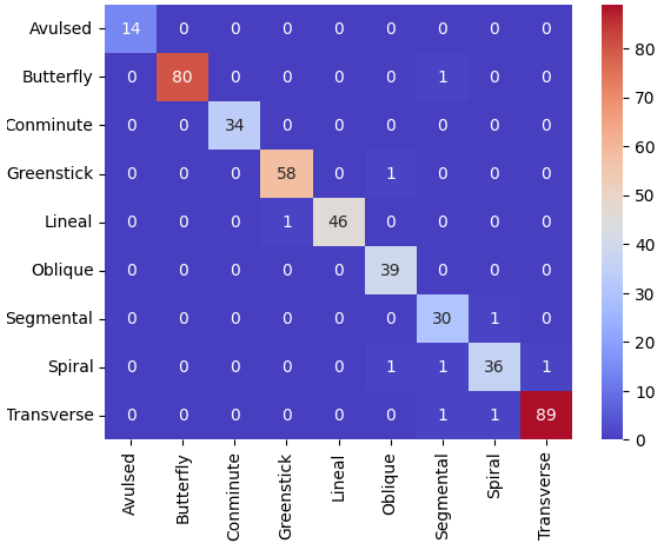

Figure 7: *Confusion matrix.*

are the worst results, although they maintain a percentage of success above 90%. In addition, we can also appreciate that the division for the tests, 20% of the total images, has been a little disproportionate since only 14 cases of the avulsed fracture have been evaluated while the butterfly and transverse fractures have been evaluated more than 80 times. However, it should be remembered that the number of patterns of each type supplied to the model was similar.

The high accuracy of 97% obtained by the deep learning model in classifying human bone fracture patterns is a significant achievement. It indicates the ability of the model to correctly identify and categorize the vast majority of fracture patterns in the evaluated dataset. In addition, attention should be focused on possible biases in the data, such as imbalances in the class distribution, which could influence the interpretation of the results. In our case, as we have generated the training dataset, we have used a similar number of patterns for each type of fracture. In this way, we have ensured that the number of images used during training did not affect the results obtained. The robustness of the model suggests its potential utility in clinical applications, where accurate fracture classification is crucial for medical decision making.

5. Conclusion and Future Work

This work shows the whole process for the acquisition of a fracture pattern for its subsequent classification. For this purpose, the first step is to reconstruct the clinical case to analyze the fractured area and extract it using curvature, normality and region growth filters to minimize user interaction as much as possible. In addition, a representation used in forensic analysis is used where aspects such as the distribution, shape and number of fracture lines in each aspect of the bone are considered.

The use of deep learning models for fracture pattern classification is of special interest in the medical field given the increasing

number of fractures in the population and the consequences they have for the population. Fracture classification is essential prior to intervention as it helps to determine the strategy to be followed. Previous works only determine the occurrence of fractures in medical images but do not identify the specific type of fracture. The proposed model has been trained with real clinical cases and images obtained through an automatic forensic analysis tool. The results show 97% accuracy in identifying and classifying the 9 fracture types.

Despite the significant achievements, there are areas that could be explored in future research to further improve their clinical application such as expanding the types of fractures to classify or optimizing the model by removing layers and observing how it evolves in the face of these changes. In addition, the model could be expanded to create a fracture imaging model of the different types treated to provide an infinite source of information with which to perform medical simulations such as fracture simulation and subsequent fracture reduction.

Acknowledgments

This work has been supported by the Ministerio de Economía y Competitividad and the European Union (via ERDF funds) through the research project DPI2015-65123-R.

References

[Bu16] BAYRAM F., UNDEFINEDAKIROĞLU M.: Diffract: Diaphyseal femur fracture classifier system. *Biocybernetics and Biomedical Engineering 36*, 1 (2016), 157–171. URL: http://dx.doi.org/10.1016/j.bbe.2015.10.003, doi:10.1016/j.bbe.2015.10.003. 2

[CBRY09] CHOWDHURY A. S., BHANDARKAR S. M., ROBINSON R. W., YU J. C.: Virtual multi-fracture craniofacial reconstruction using computer vision and graph matching. *Computerized Medical Imaging and Graphics 33*, 5 (July 2009), 333–342. URL: http://dx.doi.org/10.1016/j.compmedimag.2009.01.006, doi:10.1016/j.compmedimag.2009.01.006. 2

[CGK*07] CITAK M., GARDNER M. J., KENDOFF D., TARTE S., KRETTEK C., NOLTE L., HÜFNER T.: Virtual 3d planning of acetabular fracture reduction. *Journal of Orthopaedic Research 26*, 4 (Oct. 2007), 547–552. URL: http://dx.doi.org/10.1002/jor.20517, doi:10.1002/jor.20517. 1

[CKM*16] COHEN H., KUGEL C., MAY H., MEDLEJ B., STEIN D., SLON V., HERSHKOVITZ I., BROSH T.: The impact velocity and bone fracture pattern: Forensic perspective. *Forensic Science International 266* (Sept. 2016), 54–62. URL: http://dx.doi.org/10.1016/j.forsciint.2016.04.035, doi:10.1016/j.forsciint.2016.04.035. 3

[CKM*17a] COHEN H., KUGEL C., MAY H., MEDLEJ B., STEIN D., SLON V., BROSH T., HERSHKOVITZ I.: The influence of impact direction and axial loading on the bone fracture pattern. *Forensic Science International 277* (Aug. 2017), 197–206. URL: http://dx.doi.org/10.1016/j.forsciint.2017.05.015, doi:10.1016/j.forsciint.2017.05.015. 3, 4

[CKM*17b] COHEN H., KUGEL C., MAY H., MEDLEJ B., STEIN D., SLON V., BROSH T., HERSHKOVITZ I.: The influence of impact direction and axial loading on the bone fracture pattern. *Forensic Science International 277* (Aug. 2017), 197–206. URL: https://doi.org/10.1016/j.forsciint.2017.05.015, doi:10.1016/j.forsciint.2017.05.015. 3

[CLDMPB19] CHITTAJALLU S. M., LAKSHMI DEEPTHI MANDALANENI N., PARASA D., BANO S.: Classification of binary fracture using cnn. In *2019 Global Conference for Advancement in Technology (GCAT)* (Oct. 2019), IEEE. URL: http://dx.doi.org/10.1109/GCAT47503.2019.8978468, doi:10.1109/gcat47503.2019.8978468. 2

[CLZ*19] CHEN F., LIU J., ZHAO Z., ZHU M., LIAO H.: Three-dimensional feature-enhanced network for automatic femur segmentation. *IEEE Journal of Biomedical and Health Informatics 23*, 1 (Jan. 2019), 243–252. URL: http://dx.doi.org/10.1109/JBHI.2017.2785389, doi:10.1109/jbhi.2017.2785389. 2

[EKAK17] ERICKSON B. J., KORFIATIS P., AKKUS Z., KLINE T. L.: Machine learning for medical imaging. *RadioGraphics 37*, 2 (Mar. 2017), 505–515. URL: http://dx.doi.org/10.1148/rg.2017160130, doi:10.1148/rg.2017160130. 2

[EKZ10] EGOL K. A., KOVAL K. J., ZUCKERMAN J. D.: *Handbook of fractures*. Lippincott Williams & Wilkins, 2010. 2, 3

[FBKC*12] FEDOROV A., BEICHEL R., KALPATHY-CRAMER J., FINET J., FILLION-ROBIN J.-C., PUJOL S., BAUER C., JENNINGS D., FENNESSY F., SONKA M., ET AL.: 3d slicer as an image computing platform for the quantitative imaging network. *Magnetic resonance imaging 30*, 9 (2012), 1323–1341. doi:10.1016/j.mri.2012.05.001. 2, 3

[FSG*12] FÜRNSTAHL P., SZÉKELY G., GERBER C., HODLER J., SNEDEKER J. G., HARDERS M.: Computer assisted reconstruction of complex proximal humerus fractures for preoperative planning. *Medical Image Analysis 16*, 3 (Apr. 2012), 704–720. URL: http://dx.doi.org/10.1016/j.media.2010.07.012, doi:10.1016/j.media.2010.07.012. 2

[FSH10] FORNARO J., SZÉKELY G., HARDERS M.: *Semi-automatic Segmentation of Fractured Pelvic Bones for Surgical Planning*. Springer Berlin Heidelberg, 2010, p. 82–89. URL: http://dx.doi.org/10.1007/978-3-642-11615-5_9, doi:10.1007/978-3-642-11615-5_9. 2

[Gar61] GARDEN R. S.: LOW-ANGLE FIXATION IN FRACTURES OF THE FEMORAL NECK. *The Journal of Bone and Joint Surgery. British volume 43-B*, 4 (Nov. 1961), 647–663. URL: https://doi.org/10.1302/0301-620x.43b4.647, doi:10.1302/0301-620x.43b4.647. 1

[JDPCPCLL20] JIMENEZ-DELGADO J. J., PARRA-CABRERA G., PEREZ-CANO F. D., LUQUE-LUQUE A.: Generation and validation of osseous fracture patterns by forensic analysis. *IEEE Access 8* (2020), 211506–211525. URL: http://dx.doi.org/10.1109/ACCESS.2020.3039233, doi:10.1109/access.2020.3039233. 3

[KJ13] KRONMAN A., JOSKOWICZ L.: Automatic bone fracture reduction by fracture contact surface identification and registration. In *2013 IEEE 10th International Symposium on Biomedical Imaging* (Apr. 2013), IEEE. URL: http://dx.doi.org/10.1109/ISBI.2013.6556458, doi:10.1109/isbi.2013.6556458. 2

[KSH12] KRIZHEVSKY A., SUTSKEVER I., HINTON G. E.: Imagenet classification with deep convolutional neural networks. In *Advances in Neural Information Processing Systems* (2012), Pereira F., Burges C., Bottou L., Weinberger K., (Eds.), vol. 25, Curran Associates, Inc. URL: https://proceedings.neurips.cc/paper_files/paper/2012/file/c399862d3b9d6b76c8436e924a68c45b-Paper.pdf. 4

[LLJPPCJD21] LUQUE-LUQUE A., JIMÉNEZ-PÉREZ J. R., PÉREZ-CANO F. D., JIMÉNEZ-DELGADO J. J.: A compact representation of the bone fracture area. application to fractured bones of clinical cases. *Computer Methods in Biomechanics and Biomedical Engineering: Imaging & Visualization 10*, 5 (Jan. 2021), 476–483. URL: https://doi.org/10.1080/21681163.2020.1850365, doi:10.1080/21681163.2020.1850365. 2, 3

[LLPCJD21] LUQUE-LUQUE A., PÉREZ-CANO F. D., JIMÉNEZ-DELGADO J. J.: Complex fracture reduction by exact identification of the fracture zone. *Medical Image Analysis 72* (Aug. 2021), 102120. URL: https://doi.org/10.1016/j.media.2021.102120, doi:10.1016/j.media.2021.102120. 2

[LLZ19] LU S., LU Z., ZHANG Y.-D.: Pathological brain detection based on alexnet and transfer learning. *Journal of Computational Science 30* (Jan. 2019), 41–47. URL: http://dx.doi.org/10.1016/j.jocs.2018.11.008, doi:10.1016/j.jocs.2018.11.008. 4

[MAR*18] MEINBERG E., AGEL J., ROBERTS C., KARAM M., KELLAM J.: Fracture and dislocation classification compendium—2018. *Journal of Orthopaedic Trauma 32*, 1 (Jan. 2018), S1–S10. URL: https://doi.org/10.1097/bot.0000000000001063, doi:10.1097/bot.0000000000001063. 1, 2, 3

[MEvE*22] MINNEMA J., ERNST A., VAN EIJNATTEN M., PAUWELS R., FOROUZANFAR T., BATENBURG K. J., WOLFF J.: A review on the application of deep learning for ct reconstruction, bone segmentation and surgical planning in oral and maxillofacial surgery. *Dentomaxillofacial Radiology 51*, 7 (Sept. 2022). URL: http://dx.doi.org/10.1259/dmfr.20210437, doi:10.1259/dmfr.20210437. 2

[MKNS90] MÜLLER M. E., KOCH P., NAZARIAN S., SCHATZKER J.: *The Comprehensive Classification of Fractures of Long Bones*. Springer Berlin Heidelberg, 1990. URL: http://dx.doi.org/10.1007/978-3-642-61261-9, doi:10.1007/978-3-642-61261-9. 1, 3

[NBW*05] NEUBAUER A., BÜHLER K., WEGENKITTL R., RAUCHBERGER A., RIEGER M.: Advanced virtual corrective osteotomy. *International Congress Series 1281* (May 2005), 684–689. URL: http://dx.doi.org/10.1016/j.ics.2005.03.254, doi:10.1016/j.ics.2005.03.254. 2

[OIK*09] OKADA T., IWASAKI Y., KOYAMA T., SUGANO N., CHEN Y.-W., YONENOBU K., SATO Y.: Computer-assisted preoperative planning for reduction of proximal femoral fracture using 3-d-ct data. *IEEE Transactions on Biomedical Engineering 56*, 3 (Mar. 2009), 749–759. URL: http://dx.doi.org/10.1109/TBME.2008.2005970, doi:10.1109/tbme.2008.2005970. 2

[Pau36] PAUWELS F.: Der schenkelhalsbruch: Ein mechanisches problem. *British Journal of Surgery 23*, 92 (Apr. 1936), 874. URL: https://doi.org/10.1002/bjs.1800239227, doi:10.1002/bjs.1800239227. 1

[PCJPMV*23] PÉREZ-CANO F., JIMÉNEZ-PÉREZ J., MOLINA-VIEDMA A., LÓPEZ-ALBA E., LUQUE-LUQUE A., DELGADO-MARTÍNEZ A., DÍAZ-GARRIDO F., JIMÉNEZ-DELGADO J.: Human femur fracture by mechanical compression: Towards the repeatability of bone fracture acquisition. *Computers in Biology and Medicine 164* (Sept. 2023), 107249. URL: http://dx.doi.org/10.1016/j.compbiomed.2023.107249, doi:10.1016/j.compbiomed.2023.107249. 1

[PCPCJD22] PARRA-CABRERA G., PÉREZ-CANO F. D., JIMÉNEZ-DELGADO J. J.: Fracture pattern projection on 3d bone models as support for bone fracture simulations. *Computer Methods and Programs in Biomedicine 224* (Sept. 2022), 106980. URL: http://dx.doi.org/10.1016/j.cmpb.2022.106980, doi:10.1016/j.cmpb.2022.106980. 3, 4

[PJP14] PAULANO F., JIMÉNEZ J. J., PULIDO R.: 3d segmentation and labeling of fractured bone from CT images. *The Visual Computer 30*, 6-8 (may 2014), 939–948. URL: https://doi.org/10.1007/s00371-014-0963-0, doi:10.1007/s00371-014-0963-0. 2

[RSH19] RUIKAR D. D., SANTOSH K. C., HEGADI R. S.: Automated fractured bone segmentation and labeling from ct images. *Journal of Medical Systems 43*, 3 (Feb. 2019). URL: http://dx.doi.org/10.1007/s10916-019-1176-x, doi:10.1007/s10916-019-1176-x. 2

[SNHJ16] SABET F. A., NAJAFI A. R., HAMED E., JASIUK I.: Modelling of bone fracture and strength at different length scales: a review. *Interface Focus 6*, 1 (Feb. 2016), 20150055. URL: https://doi.org/10.1098/rsfs.2015.0055, doi:10.1098/rsfs.2015.0055. 2

[SPB*14] SMITH T., PELPOLA K., BALL M., ONG A., MYINT P. K.: Pre-operative indicators for mortality following hip fracture surgery: a systematic review and meta-analysis. *Age and Ageing 43*, 4 (June 2014), 464–471. URL: http://dx.doi.org/10.1093/ageing/afu065, doi:10.1093/ageing/afu065. 1

[SPH*19] SINTHURA S. S., PRATHYUSHA Y., HARINI K., PRANUSHA Y., POOJITHA B.: Bone fracture detection system using cnn algorithm. In *2019 International Conference on Intelligent Computing and Control Systems (ICCS)* (May 2019), IEEE. URL: http://dx.doi.org/10.1109/ICCS45141.2019.9065305, doi:10.1109/iccs45141.2019.9065305. 2

[SWS17] SHEN D., WU G., SUK H.-I.: Deep learning in medical image analysis. *Annual Review of Biomedical Engineering 19*, 1 (June 2017), 221–248. URL: http://dx.doi.org/10.1146/annurev-bioeng-071516-044442, doi:10.1146/annurev-bioeng-071516-044442. 2

[TKK*10] TOMAZEVIC M., KREUH D., KRISTAN A., PUKETA V., CIMERMAN M.: *Preoperative Planning Program Tool in Treatment of Articular Fractures: Process of Segmentation Procedure*. Springer Berlin Heidelberg, 2010, p. 430–433. URL: http://dx.doi.org/10.1007/978-3-642-13039-7_108, doi:10.1007/978-3-642-13039-7_108. 2

[VA23] VALLURUPALLI S. P., ANURADHA T.: *Bone Fracture Detection Using CNN*. Springer Nature Singapore, 2023, p. 379–386. URL: http://dx.doi.org/10.1007/978-981-99-6550-2_29, doi:10.1007/978-981-99-6550-2_29.

[VSY*19] VOON T. T., SOM M. H. M., YAZID H., BASARUDDIN K. S., SULAIMAN A. R.: Segmentation of cortical and cancellous bone with osteogenesis imperfecta using thresholding-based method. *Journal of Physics: Conference Series 1372*, 1 (Nov. 2019), 012006. URL: http://dx.doi.org/10.1088/1742-6596/1372/1/012006, doi:10.1088/1742-6596/1372/1/012006. 2

[WAT*07] WILLIS A., ANDERSON D., THOMAS T., BROWN T., MARSH J. L.: 3d reconstruction of highly fragmented bone fractures. In *Medical Imaging 2007: Image Processing* (Mar. 2007), Pluim J. P. W., Reinhardt J. M., (Eds.), SPIE. URL: http://dx.doi.org/10.1117/12.708683, doi:10.1117/12.708683. 2

[WLW*15] WANG S., LU Z., WEI L., JI G., YANG J.: Fitness-scaling adaptive genetic algorithm with local search for solving the multiple depot vehicle routing problem. *SIMULATION 92*, 7 (Sept. 2015), 601–616. URL: http://dx.doi.org/10.1177/0037549715603481, doi:10.1177/0037549715603481. 4

[YHKJEO20] YOON S.-J., HYONG KIM T., JOO S.-B., EEL OH S.: Automatic multi-class intertrochanteric femur fracture detection from ct images based on ao/ota classification using faster r-cnn-bo method. *Journal of Applied Biomedicine 18*, 4 (Dec. 2020), 97–105. URL: http://dx.doi.org/10.32725/jab.2020.013, doi:10.32725/jab.2020.013. 2

[YR20] YADAV D. P., RATHOR S.: Bone fracture detection and classification using deep learning approach. In *2020 International Conference on Power Electronics & IoT Applications in Renewable Energy and its Control (PARC)* (Feb. 2020), IEEE. URL: http://dx.doi.org/10.1109/PARC49193.2020.236611, doi:10.1109/parc49193.2020.236611. 2

[ZWX*23] ZENG B., WANG H., XU J., TU P., JOSKOWICZ L., CHEN X.: Two-stage structure-focused contrastive learning for automatic identification and localization of complex pelvic fractures. *IEEE Transactions on Medical Imaging 42*, 9 (Sept. 2023), 2751–2762. URL: http://dx.doi.org/10.1109/TMI.2023.3264298, doi:10.1109/tmi.2023.3264298. 2